Magneto-optical study of the magnetization reversal process of Fe nanowires

2002 J. Phys.: Condens. Matter 14 7525

(http://iopscience.iop.org/0953-8984/14/32/312)

INSTITUTE OF PHYSICS PUBLISHING JOURNAL OF PHYSICS: CONDENSED MATTER

J. Phys.: Condens. Matter **14** (2002) 7525–7538 PII: S0953-8984(02)36255-6

Magneto-optical study of the magnetization reversal process of Fe nanowires

Till Schmitte[1,3], Katharina Theis-Bröhl[1], Vincent Leiner[1], Hartmut Zabel[1], Siegfried Kirsch[2] and Axel Carl[2]

[1] Institut für Experimentalphysik/Festkörperphysik, Ruhr-Universität Bochum, D44780 Bochum, Germany
[2] Experimentelle Tieftemperaturphysik, Gerhard-Mercator-Universität Duisburg, D47048 Duisburg, Germany

E-mail: till.schmitte@ruhr-uni-bochum.de

Received 26 April 2002
Published 2 August 2002
Online at stacks.iop.org/JPhysCM/14/7525

Abstract

We discuss results of magneto-optical Kerr effect (MOKE) measurements performed on a thin Fe film of 13 nm thickness, which has been patterned into a periodic arrangement of nanowires by means of optical interference lithography. The resulting array of nanowires consist of stripes having a width of 150 nm and a periodicity of 300 nm. MOKE hysteresis loops are measured within magnetic fields which are aligned in different directions, both parallel and perpendicular with respect to the direction of the nanowires as well as for various angles in between. A particular arrangement of the longitudinal Kerr effect measurement allows us to identify both the longitudinal and the transverse component of the magnetization of Fe nanowires. From this both the angle and the magnitude of the magnetization vector $\vec{M}$ are derived. For a non-parallel alignment of the nanowires with respect to the direction of the external magnetic field, the hysteresis loops consist of a plateau region with two coercive fields H_{c1} and H_{c2}, which is discussed as resulting from an anisotropic pinning behaviour of magnetic domains in directions along and perpendicular to the nanowires.

1. Introduction

The understanding of the magnetization reversal process of artificially structured magnetic islands and wires is important both from a fundamental point of view and also for potential magneto-electronic device applications [1]. Of particular interest is the magnetic domain structure within these nanostructured magnetic elements, their remanent magnetization and the shape of their magnetic hysteresis loop. On the one hand, these parameters primarily depend on both the shape and the aspect ratio of the magnetic elements and, on the other

[3] URL: http://www.ep4.ruhr-uni-bochum.de.

hand, they depend on the intrinsic magnetic anisotropy constants of the magnetic material used [2]. In particular, if magnetic islands or wires are separated by only small distances, long-range magnetic dipole interaction between the elements also has to be taken into account [3]. Typical techniques for nanostructuring, such as electron-beam lithography (EBL), allow one to fabricate well defined magnetic elements [4] and also magnetic wires [3] showing interesting magnetic behaviour. However, the drawback of EBL and similar techniques is that the size of the area to be patterned is usually limited to some fractions of a square millimetre, whereas for technical applications it is necessary to pattern much larger areas. This may be achieved by using self-organizing processes [5] or e.g. the atomic saw method [6]. Another feasible technique is optical interference lithography [7, 8], which allows one to periodically pattern large areas (several square centimetres) with well defined periodicities.

Magnetic domain structures as well as the magnetization reversal process of nanostructured magnetic elements may be investigated by a number of experimental methods. On the one hand, magnetic domains of single magnetic elements may be imaged in real space by various techniques such as Kerr microscopy [2], Lorentz microscopy [9], scanning electron microscopy with polarization analysis (SEMPA) [10], x-ray magnetic circular dichroism (XMCD) microscopy [11] and magnetic force microscopy (MFM) [12]. Hysteresis loops of magnetic elements are derived by evaluating the total size of magnetic domains having a particular direction of the magnetization vector with respect to the direction of the applied magnetic field. Also, the hysteresis loop of single-domain magnetic elements may be measured with MFM, by using a calibrated MFM tip [13]. On the other hand, hysteresis loops of magnetic elements may as well be measured via magneto-optical Kerr effect (MOKE), superconducting quantum interference device (SQUID) magnetometry or vibrating sample magnetometry (VSM) for which the magnetization reversal process may as well be identified from the shape of the corresponding hysteresis loop. However, resolution and accuracy of the latter techniques ask for a large number of identical elements to be investigated in parallel, such that the hysteresis loop obtained yields information upon the *average* magnetization reversal process of all elements, and not just upon the magnetization reversal of a single element. Nevertheless, such techniques more easily allow for hysteresis loop measurements taken at various angles, e.g. in orthogonal directions, from which the *vector* of the magnetization can be reconstructed. For the present investigation we have utilized the MOKE, since this technique is particularly suited in view of the above-mentioned advantages. Thus, it can easily be operated like a vector magnetometer. In addition to the longitudinal MOKE geometry, we have also measured the perpendicular component of the magnetization of nanowires by applying an external magnetic field in a direction normal to the plane of incidence. Both the longitudinal and the perpendicular field orientation allows us to derive a vector model for the magnetization process, following previous work by Daboo *et al* [14].

2. Experimental details

The sample under investigation is a thin Fe film of 13 nm thickness which has been transformed into a periodic nanowire array by an anisotropic plasma etching process after film deposition. The Fe film was grown within a UHV-MBE system on a 1.7 cm × 1.7 cm $Al_2O_3(1\bar{1}02)$ (r-plane) substrate onto a 150 nm thick Nb buffer layer, which has a (001) orientation as can be derived from the three-dimensional epitaxial relationship between niobium and sapphire [15] and as was measured by x-ray scattering. The Fe growth temperature was 120 °C. From the formation of epitaxial Fe(110) films on Nb(110) at the same substrate temperature [16] one would expect the formation of epitaxial Fe(001) on Nb(001). This is not the case, as was found from x-ray scattering experiments. Instead, a polycrystalline film growth was indeed required in order to

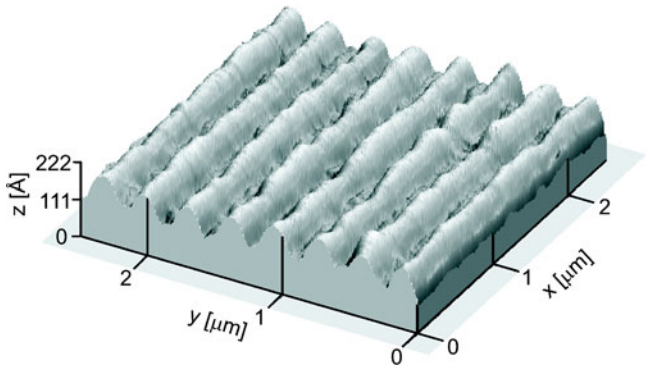

Figure 1. Surface morphology of a periodic array of Fe nanowires on a Nb/sapphire substrate imaged with AFM. The three-dimensional surface graph covers a region of $2.5 \times 2.5\ \mu m^2$.
(This figure is in colour only in the electronic version)

reduce the intrinsic magnetic in-plane anisotropy for reasons discussed below. The Fe film was additionally covered with a 4 nm thick Nb film in order to protect it against oxidation. Both the thickness and the roughness of the film were analysed by x-ray reflectometry. After film preparation, the sample was spin coated with a positive photoresist. The resist was then exposed by a periodic line pattern created by interference of a split laser beam (wavelength of 457.8 nm) by using a Michelson-type interferometer set-up [17]. Subsequently, the resist was developed, resulting in a periodically modulated resist mask on top of the Fe film with a cosine-squared thickness modulation of 300 nm periodicity. The sample was then ion etched in a conventional rf-sputtering system, using the modulated resist as an etching mask. During the sputtering process, the etching rate of the resist is $\approx$10 times higher than that of the Fe film. Therefore, the thickness of the resist mask was chosen such that it was initially about 10 times thicker than the metal film. As a result of the etching process, the periodically structured resist mask is transferred into the underlying Fe film, so we finally obtain an array of well separated Fe wires on top of a Nb buffer. After lift-off of the remains of the resist we checked the quality of the sample by imaging its surface morphology with an atomic force microscope (AFM). Figure 1 shows a corresponding AFM image of $2.5 \times 2.5\ \mu m^2$ size. The measurement confirms

(i) the regularity of the Fe nanowires having a width of $\approx$150 nm and a periodicity of 300 nm and
(ii) that the wires are completely separated from each other.

Note that the stripes have a sinusoidal shape, which is a consequence of the lithography technique used.

Hysteresis loop measurements were performed by using a high-resolution MOKE set-up in the longitudinal configuration with s-polarized light, which is well suited for measuring the exact Kerr angle as a function of the applied magnetic field. More details of the experimental set-up can be found in [18]. In the longitudinal configuration the magnetic field is directed along the plane of incidence and the measured Kerr angle is proportional to the component of the magnetization vector along the field direction, $\theta_K^l \propto m_l$, where m_l is the longitudinal component of $\vec{M}$ in a projection parallel to $\vec{H}$. In addition, the experimental set-up allows for a rotation of the sample around its surface normal (angle χ) in order to apply a magnetic field in various in-plane directions. Hysteresis measurements in only this configuration do not allow one to distinguish between a magnetization reversal via domain rotation and/or via domain

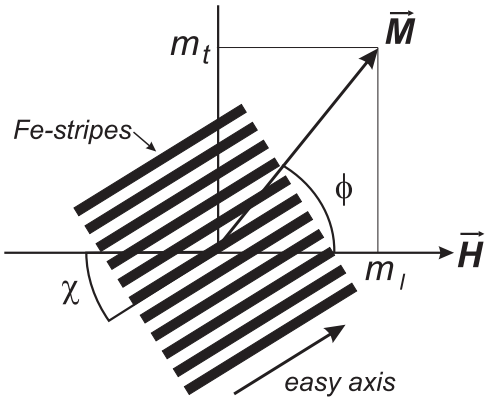

Figure 2. Definition of the sample rotation χ and the angle ϕ of the magnetization vector $\vec{M}$ for the case of the longitudinal set-up. In order to measure the transverse magnetization component m_t, the field and the sample are rotated by 90°, such that the angle χ is kept constant, but the magnetization component m_t is in the plane of incidence.

formation and wall motion. Therefore, we have also performed MOKE measurements with the external magnetic field oriented perpendicular to the plane of incidence. In this so-called perpendicular configuration the MOKE measures the magnetization component parallel to the plane of incidence but perpendicular to the magnetic field, $\theta_K^t \propto m_t$. The configuration of the experimental set-up is sketched in figure 2.

Both components of the magnetization, m_l and m_t, yield the vector sum of the average magnetization vector $\vec{M}$ as measured within a region, which is illuminated by the laser spot. This area measures $\approx$1 mm^2. The magnetization vector can then be written as

$$\vec{M} = \begin{pmatrix} m_l \\ m_t \end{pmatrix} = |M| \begin{pmatrix} \cos\phi \\ \sin\phi \end{pmatrix}. \tag{1}$$

The constant of proportionality between the Kerr angle θ_K and the two magnetization components is *a priori* unknown and it is not necessarily the same for the longitudinal and the transverse cases. However, for the present sample it is found that the saturation Kerr angle is independent of the sample rotation χ, i.e. if the sample is magnetically saturated in a direction either parallel or perpendicular to the wire axis. Furthermore, the angle of incidence was kept constant in both configurations at about 40°. Thus, for the following analysis we assume that the proportionality constant is the same for both configurations, perhaps including a small error which, however, should be tolerable. Another potential source of error may arise from the polar MOKE effect, which is left out in our present investigation. Such a contribution would result from a magnetization component oriented perpendicular to the sample surface. As shown below, however, the film magnetization is oriented almost perfectly in-plane, leading to a vanishing contribution of the polar MOKE effect. Also, any second-order magneto-optical effects [19] are neglected in our analysis. Then, we may write

$$\frac{m_l}{m_t} = \frac{\cos\phi}{\sin\phi} = \frac{\theta_K^l}{\theta_K^t}, \tag{2}$$

from which follows the angle of rotation ϕ of the magnetization vector:

$$\phi = \arctan\left(\frac{\theta_K^t}{\theta_K^l}\right). \tag{3}$$

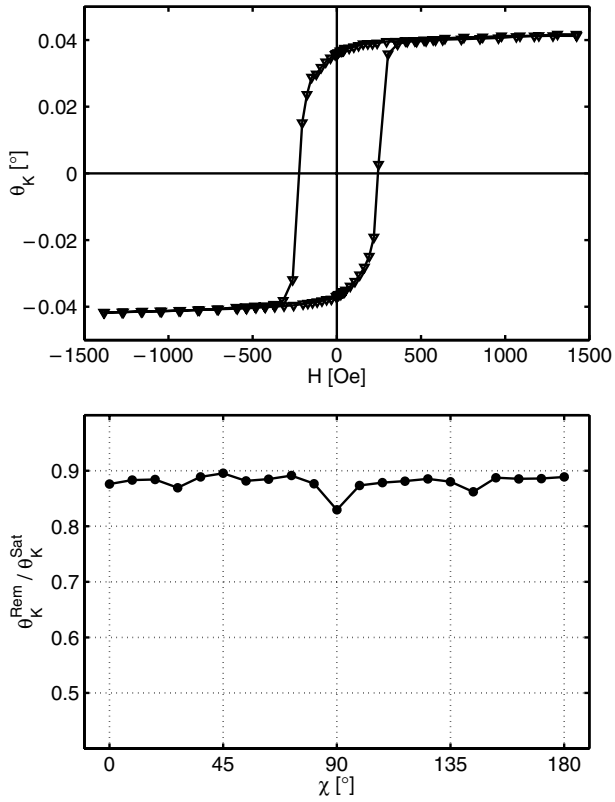

Figure 3. The MOKE hysteresis loop of the unpatterned thin Fe film (upper panel). The lower panel depicts the results of MOKE hysteresis loop measurements as a function of the angle of rotation of the unpatterned sample, where θ_K^{rem} as measured at remanence is normalized to θ_K^{sat} as measured at saturation, and plotted as a function of the angle of rotation χ, which is a measure of the magnetic anisotropy.

Furthermore, we may express $|M|$, normalized to the saturation magnetization, as

$$\frac{|M|}{|M|^{sat}} = \frac{\theta_K^l}{\theta_K^{l,sat}} \frac{1}{\cos\phi}. \tag{4}$$

Within the experiment, first the sample is put into the longitudinal configuration and hysteresis loops are measured for various in-plane rotation angles χ using increments of $\Delta\chi = 9°$. The measurements are then repeated with the same angles of rotation but for the transverse configuration. For both configurations, $\chi = 0°$ is defined as the angle for which the external magnetic field is aligned parallel to the Fe stripes (see figure 2) with an uncertainty of $\pm 2°$, which results from the redefinition of the angle χ when the experimental set-up is modified from the longitudinal to the transverse configuration.

3. Experimental results

3.1. Magnetic properties of the continuous Fe film

After film deposition and before plasma etching of the stripes we carried out reference MOKE measurements on the continuous Fe film. The upper panel of figure 3 presents a typical MOKE

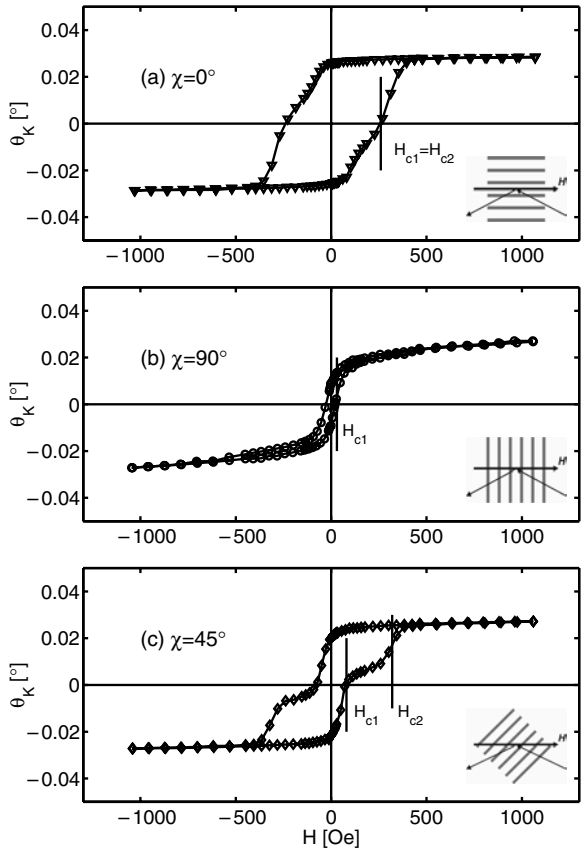

Figure 4. MOKE hysteresis loops as measured in the longitudinal configuration. (a) The external magnetic field is oriented parallel to the nanowires, $\chi = 0°$; (b) the magnetic field is oriented perpendicular to the nanowires, $\chi = 90°$; (c) the nanowires are rotated by an angle of 45° with respect to the direction of the external field. The insets depict correspondingly the orientation of the stripes with respect to the directions of both the external magnetic field H and the reflected laser beam.

hysteresis loop. The lower panel shows the Kerr rotation measured at remanence normalized to the Kerr rotation in saturation as a function of the angle of rotation χ about the surface normal of the Fe film. As can be readily seen from figure 3, the remanent magnetization amounts to about 88% of the saturation magnetization and it is almost independent of the angle of rotation. Thus, the overall in-plane magnetic anisotropy is indeed negligible, as was what we intended by choosing the above-mentioned growth conditions during film deposition. The coercive field of the continuous film is $H_c = 250$ Oe, as is typical for a polycrystalline Fe film containing many grain boundaries. Therefore, the Fe film is a good candidate for use in the investigation of an induced magnetic anisotropy caused by a lithographic patterning process.

3.2. Magnetic properties of the Fe nanowire array: longitudinal component

Figure 4 shows three typical MOKE hysteresis loops taken for the array of Fe nanowires with different in-plane angles χ as measured in the longitudinal configuration. The hysteresis loop in (a) has been recorded with the external magnetic field oriented parallel to the wires. In this

case, we find an almost square hysteresis loop with a relatively large coercive field H_c, which represents the typical behaviour of a sample when magnetically saturated along an easy axis of the magnetization. The coercive field $H_c = 250$ Oe indeed matches the value determined for the continuous film. However, the absolute values of the Kerr rotation in saturation are reduced when compared to the unpatterned film. This simply results from the fact that less material contributes to the measured signal in the case of the patterned film. Note also that the slope of the hysteresis loop at H_c is less steep for the structured sample in comparison to the unpatterned film. This indicates that the magnetization reversal is dominated by a different switching mechanism. Moreover, the patterning process obviously leads to an increase of the absolute value of the remanence in the easy direction (parallel to the wires) suggesting a suppression of domain formation.

Figure 4(b) shows the corresponding hysteresis loop for the Fe nanowire sample after the sample was rotated by 90°, i.e. when the Fe wires were oriented perpendicular to both the external field and the plane of incidence. Here, a typical hard axis hysteresis loop is obtained. The coercive field reduces to $H_c = 50$ Oe and the saturation field increases to values beyond 1000 Oe, which is the maximum magnetic field value of the present experimental set-up.

Figure 4(c) shows a MOKE hysteresis loop taken for an intermediate angle of rotation $\chi = 45°$. The hysteresis loop clearly exhibits a step-like behaviour, when the direction of the external field is reversed after saturation.

Some characteristic features of the hysteresis loops shown in figure 4 are presented in figure 5 as a function of the angle of rotation χ. Figure 5(a) shows the remanent Kerr signal θ_K^{rem} normalized to the Kerr signal at saturation θ_K^{sat} as a function of χ, which yields information about the squareness of the hysteresis loops. According to figure 5(a) the remanent Kerr signal is reduced significantly at certain angles χ without reaching zero-values signifying the hard axis orientations (around 90° and 270°). For the corresponding angles χ along the easy axis orientations (0° and 180°) the ratio $\theta_K^{rem}/\theta_K^{sat}$ measures almost unity. Similar behaviour is obtained when the coercive field H_c is plotted as a function of the angle of rotation χ in figure 5(b), from which we find two pronounced minima of χ at around 90° and 270°. The small local maxima within the minima at 90° and 270° reflect small changes of the anisotropy which are also found in the continuous film at these angles (compare the lower panel of figure 3). The hysteresis loops measured for intermediate angles of rotation χ exhibit steps, which occur at characteristic magnetic fields H_{c2}. Figure 5(c) shows H_{c2} as a function of the angle of rotation χ. H_{c2} exhibits maxima at the hard axes directions at 90° and 270°.

As mentioned above, hysteresis loops which are measured at intermediate angles of rotation show certain steps at magnetic fields H_{c2}. Some of those hysteresis loops are displayed again in figure 6 on an enlarged scale, where we have plotted only half of the hysteresis loops as measured in longitudinal configuration. Obviously, H_{c2} almost coincides with H_{c1} when measured along the easy axis ($\chi = 0°$; see figure 4(a)) and starts to increase when the sample is rotated away from the easy axis (see figure 6). Finally, H_{c2} fades out into the region of saturation when $\chi = 90°$. Note that θ_K^l-values in between H_{c1} and H_{c2} increase from almost zero to the saturation Kerr rotation which is measured in the direction of the hard axis. Note also that even the hysteresis loop measured at $\chi = 0°$ (figure 4(a)) reveals a small step in the vicinity of the coercive field.

From the results of longitudinal MOKE measurements with the magnetic field direction within the plane of incidence we may indeed conclude that patterning of the thin Fe film into an array of nanowires induces a strong uniaxial anisotropy, which results from the shape anisotropy of Fe nanowires. The saturation field measured with MOKE along the hard axis is rather high, exceeding 1000 Oe.

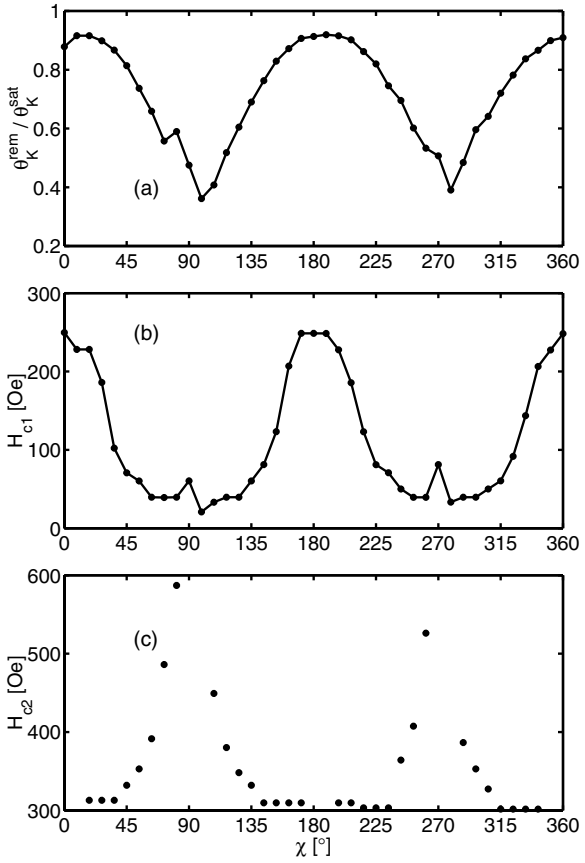

Figure 5. Results from hysteresis loop measurements at different angles of rotation χ: (a) Kerr rotation as measured at remanence normalized to the Kerr rotation as measured at saturation, (b) coercive field H_{c1} and (c) the position of steps in the hysteresis loops measured at intermediate angles of rotation between the hard axis and the easy axis (H_{c2}).

3.3. Magnetic properties of the Fe nanowire array: transverse component

As discussed above, we have also determined the transverse component of the magnetization vector by Kerr effect measurements. Corresponding hysteresis loops for three directions of the external magnetic field relative to the direction of the Fe nanowires are shown in figure 7. The hysteresis loop reproduced in figure 7(a) was measured within a magnetic field direction parallel to the Fe nanowires, i.e. along the easy axis of the magnetization. Ideally, within this configuration the measured Kerr rotation should remain zero unless certain components of the magnetization are directed along the plane of incidence during the magnetization reversal process. As can be seen from figure 7(a), the measured Kerr rotation is indeed almost zero. A small signal is seen with a maximum value at zero field. The origin of this behaviour will be discussed below. The coercive field is the same as measured for the easy direction in the longitudinal configuration. Figure 7(b) shows the hysteresis loop for a magnetic field pointing along the hard axis direction, i.e. in a direction perpendicular to the wires and the plane of incidence. In this configuration the measured Kerr rotation is larger than in the previous case and non-zero up to the highest field values. From this behaviour we infer that the sample could

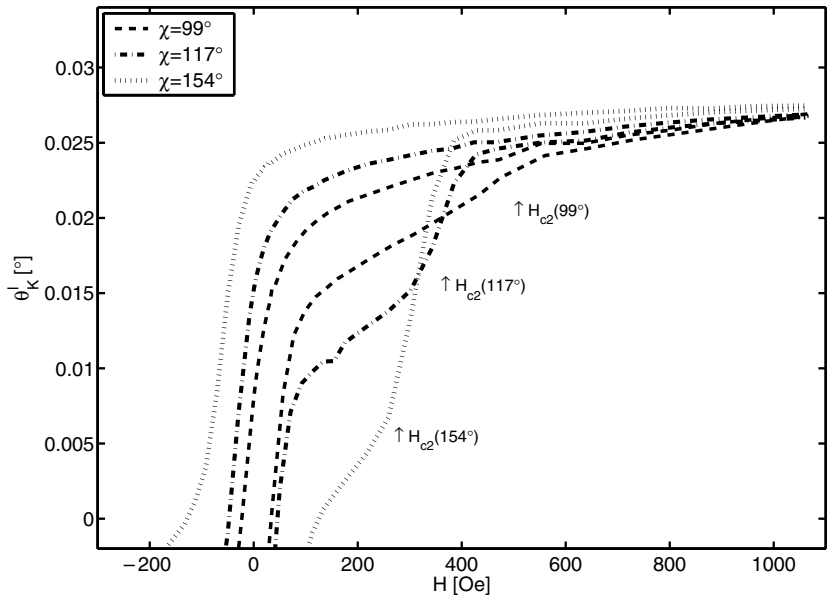

Figure 6. Evolution of the characteristic magnetic field H_{c2} as a function of the angle of rotation χ. Different curve shapes represent typical hysteresis loops as taken in the longitudinal configuration for intermediate angles of rotation. $\chi = 99°$ is close to the hard axis direction, i.e. when the external field is applied perpendicular to the nanowires.

not be magnetically saturated in the hard axis direction, in agreement with the result shown in figure 4(b). Both measurements therefore represent minor loop measurements.

Figure 7(c) shows the transverse component of the Kerr rotation measured for an angle of rotation of $\chi = 45°$. Also here, the hysteresis loop exhibits steps similar to the ones shown in figure 4(c). Note that the coercive field, denoted here as H_{c2}, is almost identical with the switching field H_{c2} as defined in the previous section for the longitudinal magnetization component.

According to the MOKE hysteresis shown in figure 7(a), the transverse magnetization component never reaches zero even at high magnetic fields, indicating that the sample is never fully saturated in the present set-up. This also corresponds to the hysteresis loop measurements in the longitudinal configuration, for which we always find a small final slope in the high-field region, even in the easy axis configuration (figure 4(a)). The reason for this may be the presence of canted spins, which may result from the rough surface of the sample. In addition, this effect may be pronounced within our measurement through the high surface sensitivity of the MOKE method.

4. Analysis and discussion

The results of MOKE hysteresis loop measurements as a function of the sample rotation and expressed in terms of the longitudinal and transverse component of the magnetization can be combined in order to calculate the angle and magnitude of the magnetization vector by using equations (3) and (4). The corresponding results of such an analysis are displayed in figure 8, which provides an overview of the magnetization reversal process of the Fe nanowires. Here, two ideal cases can easily be distinguished. If the angle of the magnetization vector changes

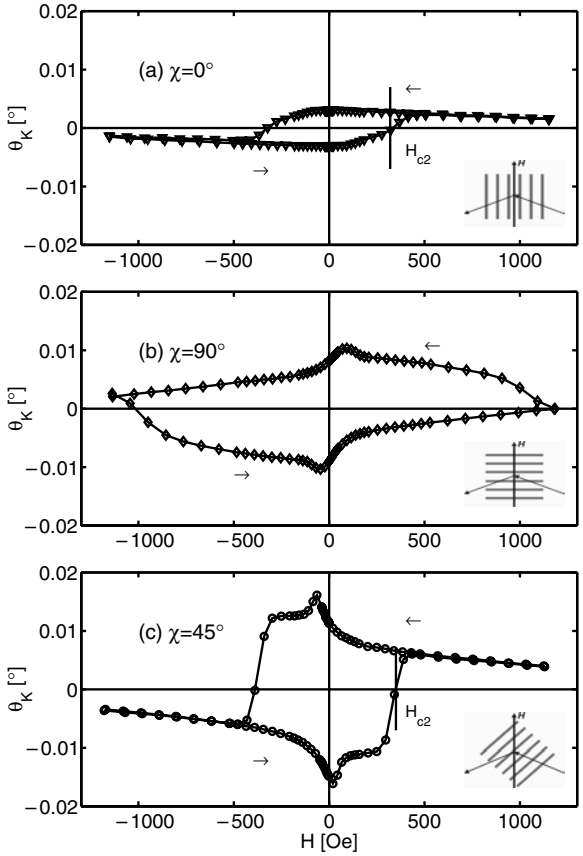

Figure 7. MOKE hysteresis loops with the magnetic field oriented perpendicular to the plane of incidence, which probes the transverse component of the magnetization: (a) the array of Fe nanowires is aligned parallel to the direction of the external magnetic field (easy axis configuration); (b) the magnetic field is applied perpendicular to the array of nanowires (hard axis configuration); (c) the field is oriented at 45° to the Fe nanowires (intermediate configuration). The insets depict the orientation of the stripes with respect to both the external magnetic field H and the reflected laser beam. Note that the θ_K-scale is divided by two in comparison with what is shown in figure 4 for the longitudinal configuration.

without changing the magnitude $|M|$, then the magnetization reversal occurs via coherent rotation. On the other hand, if the angle of the magnetization vector remains constant within a certain magnetic field range but the magnitude $|M|$ changes, then magnetic domains are formed.

Firstly, we discuss the magnetization reversal with the magnetic field oriented parallel to the Fe nanowires (figures 8(a), (b)), i.e. when the magnetic field is directed along the easy axis of the nanowires having a twofold magnetic anisotropy. When the magnetic field is swept from negative to positive values, the magnetization vector within the Fe nanowires remains parallel to the direction of the external field ($\phi = 0°$ in figure 8(a)), until the magnetic field reaches a value which matches the coercive field for the easy axis $H_{c1}^{e.a.} \approx +250$ Oe. Then, $\vec{M}$ suddenly flips from 0° to 180° and further on remains parallel to the external magnetic field direction up to the highest magnetic field values. Upon reduction of the magnetic field value and subsequent reversal of the magnetic field direction the magnetization vector again rotates but in the opposite

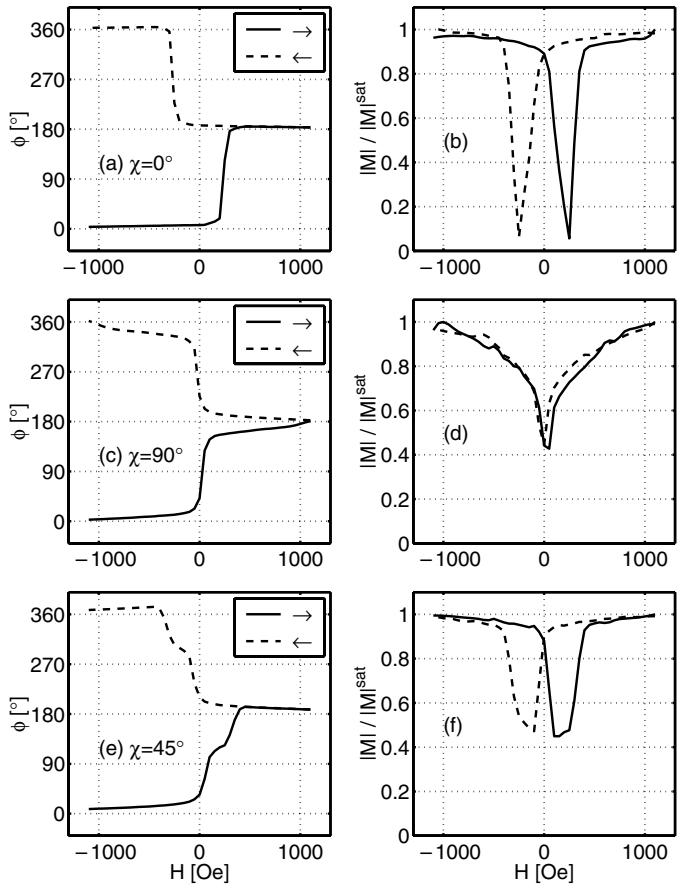

Figure 8. Conversion of the results of MOKE measurements from figures 4 and 7 by using equations (3) and (4) into the angle of the magnetization vector (left column) and the magnitude of the magnetization (right column). (a) and (b) display the results for the external magnetic field directed along the Fe nanowires (the easy axis); (c) and (d) show the results as obtained for $\vec{H}$ perpendicular to the direction of the Fe nanowires (the hard axis); in (e) and (f) the magnetic field is tilted by 45° with respect to the direction of the Fe nanowires. The solid curves represent the measurements with the magnetic field increased from negative to positive fields; the dashed curves correspond to measurements with the magnetic field decreased from positive to negative field values.

sense and reaches $\phi = 360°$ after passing the coercive field at $H_{c1}^{e.a.} \approx -250$ Oe. Both the starting point ($\phi = 0°$) and the end point ($\phi = 360°$) are degenerate. The plot of the magnitude of $\vec{M}$ normalized to the saturation value $\vec{M}^{sat}$ in figure 8(b) shows a decrease of $|M|$ over a relatively wide magnetic field range, reaching almost zero around $\pm H_{c1}^{e.a.}$. This indicates that the magnetization reversal process around $H_{c1}^{e.a.}$ is dominated by domain formation within a wide magnetic field range. The shape of $|M|(H)$ suggests that a number of domains nucleate along the nanowires, rather than just one single domain wall travelling along each wire during the magnetization reversal process. A single domain would result in a much narrower range over which $|M|$ switches.

The situation changes when the magnetic field is directed perpendicular to the nanowires, i.e. along the hard axis direction, as shown in figures 8(c) and (d). Here, the magnitude of the

magnetization $|M|$ starts to decrease as soon as the magnetic field is reduced from its maximum value. At the same time the magnetization starts to change its direction. When approaching the coercive field for the hard axis orientation $H_{c1}^{h.a.} = \pm 75$ Oe, the magnitude of the magnetization drops in an even more rapid fashion, albeit it also does not reach zero as in the previous case. Thus, for this case we assume that a number of domains are formed along the wires immediately after leaving the saturation state, most likely as a result of large demagnetizing fields. Clearly the possibility that coherent rotation is the relevant magnetization reversal mechanism can be excluded; however, some rotational processes still remain active close to the coercivity. Around H_{c1} the angle of the magnetization changes rapidly (figure 8(c)). This indicates the switching of domains which are oriented parallel to the field but perpendicular to the wire axis.

The hysteresis loops as measured in both the hard and easy directions also differ significantly from each other in terms of coercivity. Whereas H_{c1} for the easy axis loop more or less reproduces the value of the unpatterned film, its value strongly reduces for the hard axis loop. Obviously, patterning of the continuous Fe film does not change the pinning behaviour of domains along the wire axis. However, for the hard axis orientation the domain walls parallel to the external field only have to move from one side of the wires to the other side, which is probably aided by the rounded shape of the wires, thus leading to much smaller coercivities.

When the magnetic field is oriented at 45° with respect to the Fe nanowires, we expect to obtain a combination of the easy and hard axis behaviour. Both the angle and the magnitude of the magnetization vector are plotted for this case in figures 8(e) and (f). Starting at saturation within negative magnetic field values towards zero magnetic field, the direction of $\vec{M}$ changes from 0° to almost 45°, while the magnitude of $\vec{M}$ only slightly decreases. Within this first part of the hysteresis loop the situation is comparable to what is found for the hard axis loop. Magnetic domains are nucleated along the nanowires, which are oriented in only one direction, because the external magnetic field has a component parallel to the wires. Close to H_{c1} the remaining domains, which are still oriented parallel to the external field, switch by 180°, resulting in a decrease of the magnitude of $\vec{M}$. A further increase of the magnetic field leads to a metastable situation within the plateau region between H_{c1} and H_{c2}. Here, some of the domains appear to be oriented parallel to the field and some domains are oriented parallel to the stripes. This can be verified from the fact that the orientation of $\vec{M}$ is almost perpendicular to the stripes, and the magnitude of $\vec{M}$ is reduced to $\approx\frac{1}{2}$ of its saturation value. Only after application of a magnetic field larger than H_{c2} does the magnetization switch into a direction parallel to the magnetic field direction and the magnitude regain its saturation value. The domains which are oriented parallel to the nanowires switch their direction, comparable to the case of the easy axis loop.

The above interpretation for the three main orientations of the Fe nanowires with respect to the direction of the magnetic field (0°, 90° and 45°) is consistent with measurements taken in various other in-plane directions. Figure 5(c) displays H_{c2} as a function of the direction of the external field. H_{c2} increases when approaching the hard axes directions (90° and 270°), and it is small otherwise. This can be explained by the corresponding component of the external magnetic field that drives the switching process. For instance, close to the hard axis orientation the external magnetic field component along the stripes becomes small; therefore, a higher external field is required to switch the domains which are oriented parallel to the nanowires. This can be expressed approximately through the relation: $H_{c2} = H_c^{e.a.}/\cos\chi$.

The true domain structure of the nanowires is likely to be affected by the morphology of the stripes. In particular, it might by affected by their waviness and by the fluctuations of the wire width and wire height. Future MFM investigations or spin-polarized scanning tunnelling microscopy [20] will help to identify the domain structure of the Fe nanowires. It should be

mentioned that in contrast to the case for the data presented in [3], here no evidence for a dipolar interaction between the wires could be discerned. This, however, most likely results from the fact that the separation of the nanowires is of the same magnitude as the wire width.

5. Conclusions

With an analysis of magneto-optical hysteresis loop measurements taken for both longitudinal and transverse configurations we have demonstrated the complex magnetization reversal behaviour of an array of Fe nanowires. The Fe nanowires were fabricated by patterning a continuous polycrystalline Fe film by using optical interference lithography. Before patterning, essentially no in-plane magnetic anisotropy could be detected for the continuous Fe film. The pattering process induces a uniaxial magnetic anisotropy with the easy axis of magnetization directed parallel to the nanowires.

Due to the imposed shape anisotropy of the Fe nanowire array, the magnetization reversal behaviours are expected to be quite different for magnetic field orientations parallel and perpendicular to the nanowires. We have investigated the magnetization reversal properties of the nanowires by analysing both the transverse and the longitudinal components of the magneto-optical Kerr rotation. For a magnetic field orientation parallel to the nanowires we observe easy axis behaviour of the magnetization reversal which is dominated by domain nucleation. For the magnetic field oriented perpendicular to the nanowires the magnetization reversal is found to be also dominated by domain nucleation but with different pinning potentials for magnetic domains magnetized either parallel or perpendicular to the wire axis, leading to smaller coercivities for the latter. For intermediate orientations of the magnetic field with respect to the direction of nanowires (between hard and easy axis), a superposition of the two magnetization reversal processes is found, resulting in a plateau-like region in the hysteresis loop due to a metastable domain configuration. In summary, our analysis shows the potential usage of a vector magnetometer in order to unveil the complex magnetization reversal processes of nanoscaled magnetic wire arrays.

Acknowledgment

This work was supported by *SFB 491* of the Deutsche Forschungsgemeinschaft: 'Magnetic Heterostructures: Structure and Transport', which is gratefully acknowledged.

References

[1] Prinz G and Hathaway K 1995 *Phys. Today* **4** 24
[2] Hubert A and Schäfer R 1998 *Magnetic Domains* (Heidelberg: Springer)
[3] Shearwood C, Blundell S J, Daird M J, Bland J A C, Gester M, Ahmed H and Hughes H P 1994 *J. Appl. Phys.* **75** 5249
[4] Yu J, Rüdiger U, Kent A B, Thomas L and Parkin S S P 1999 *Phys. Rev.* B **60** 7352
[5] Sun S H, Murray C B, Weller D, Folks L and Moser A 2000 *Science* **272** 85
[6] Jaffres H, Ressier L, Peyrade J P, Fert A R, Gogl P, Thiaville A, Schuhl A and Nguyen Van Dau F 1998 *J. Appl. Phys.* **84** 4375
[7] Savas T A, Shah S N, Schattenburg M L, Carter J M and Smith H I 1995 *J. Vac. Sci. Technol.* B **13** 2732
[8] Wassermann E F, Thielen M, Kirsch S, Pollmann A, Weinforth H and Carl A 1998 *J. Appl. Phys.* **83** 1753
[9] Chapman J N, Johnston A B, Heydermann L J, McVitie S, Nicholson W A P and Bormans B 1994 *IEEE Trans. Magn.* **30** 4479
[10] Oepen H P and Kirschner J 1991 *Scanning Microsc.* **5** 1
[11] Fischer P, Eimuller T, Schütz G, Schmahl G, Guttmann P and Bayreuther G 1999 *J. Magn. Magn. Mater.* **198** 624

[12] Schmidt J, Skidmore G, Foss S, Dan Dahlberg E and Merton C 1998 *J. Magn. Magn. Mater.* **190** 81
[13] Lohau J, Kirsch S, Carl A and Wassermann E F 2000 *Appl. Phys. Lett.* **76** 3094
[14] Daboo C, Hicken R J, Gu E, Gester M, Gray S J, Eley D E P, Ahmad E, Bland J A C, Poessl R and Chapman J N 1995 *Phys. Rev.* B **51** 15 964
[15] Wildes A, Mayer J and Theis-Bröhl K 2001 *Thin Solid Films* **7** 401
[16] Mühge Th, Theis-Bröhl K, Westerholt K, Zabel H, Garifyanov N N, Goryunov Yu V, Garifullin I A and Khaliullin G G 1998 *Phys. Rev.* B **57** 5071
[17] Carl A, Kirsch S, Lohau J, Weinforth H and Wassermann E F 1999 *IEEE Trans. Magn.* **35** 3106
[18] Zeidler Th, Schreiber F, Zabel H, Donner W and Metoki N 1996 *Phys. Rev.* B **53** 3256
[19] Osgood R M, Clemens B M and White R L 1997 *Phys. Rev.* B **55** 8990
[20] Pietzsch O, Kubetzka A, Bode M and Wiesendanger R 2000 *Phys. Rev. Lett.* **84** 5212